

Measurement of the branching fraction of $D^+ \rightarrow \tau^+ \nu_\tau$

The BESIII collaboration



E-mail: BESIII-publications@ihep.ac.cn

ABSTRACT: By analyzing e^+e^- collision data with an integrated luminosity of 7.9 fb^{-1} collected with the BESIII detector at the center-of-mass energy of 3.773 GeV , the branching fraction of $D^+ \rightarrow \tau^+ \nu_\tau$ is determined as $\mathcal{B} = (9.9 \pm 1.1_{\text{stat}} \pm 0.5_{\text{syst}}) \times 10^{-4}$. Taking the most precise result $\mathcal{B}(D^+ \rightarrow \mu^+ \nu_\mu) = (3.981 \pm 0.079_{\text{stat}} \pm 0.040_{\text{syst}}) \times 10^{-4}$, we determine $R_{\tau/\mu} = \Gamma(D^+ \rightarrow \tau^+ \nu_\tau)/\Gamma(D^+ \rightarrow \mu^+ \nu_\mu) = 2.49 \pm 0.31$, achieving a factor of two improvement in precision compared to the previous BESIII result. This measurement is in agreement with the standard model prediction of lepton flavor universality within one standard deviation.

Contents

1	INTRODUCTION	1
2	BESIII DETECTOR AND MONTE CARLO SIMULATION	2
3	EVENT SELECTION AND DATA ANALYSIS	3
4	DETERMINATION OF THE BRANCHING FRACTION	5
5	SYSTEMATIC UNCERTAINTIES	6
6	SUMMARY	7

1 INTRODUCTION

Lepton Flavor Universality (LFU), a fundamental assumption of the Standard Model (SM), asserts that leptons from different generations possess identical coupling to gauge bosons [1]. The leptonic decays of the D^+ meson present an excellent opportunity for testing $\mu - \tau$ LFU. Figure 1 shows the Feynman diagram of the $D^+ \rightarrow \ell^+ \nu_\ell$ ($\ell = e, \mu, \tau$) decays at tree level, in which the c quark and the \bar{d} quark annihilate, followed by a weak current connecting to the system of the lepton ℓ^+ and the corresponding flavored neutrino ν_ℓ . Throughout this paper, charge conjugate channels are implied.

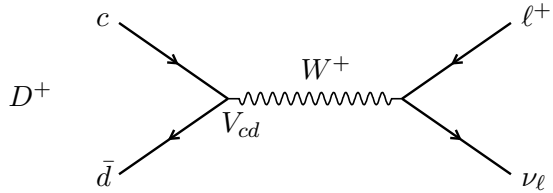


Figure 1. Tree level Feynman diagram of the leptonic decay of the D^+ meson. The CKM matrix element, V_{cd} , appears at the decay vertex.

Due to the isolation of the hadronic and leptonic systems, the partial decay width of $D^+ \rightarrow \ell^+ \nu_\ell$ to the lowest order within the SM is proportional to the product of the decay constant f_{D^+} and the Cabibbo-Kobayashi-Maskawa (CKM) matrix element $|V_{cd}|$, given in a simple form [1–3]:

$$\Gamma(D^+ \rightarrow \ell^+ \nu_\ell) = \frac{G_F^2 f_{D^+}^2}{8\pi} |V_{cd}|^2 M_{\ell^+}^2 M_{D^+} \left(1 - \frac{M_{\ell^+}^2}{M_{D^+}^2}\right)^2, \quad (1.1)$$

where M_ℓ and M_{D^+} are the masses of the lepton ℓ and the D^+ meson, respectively. The partial decay width is the branching fraction divided by the D^+ lifetime. G_F is the Fermi coupling constant, which is known to high precision. From Eq. 1.1 and assuming LFU, the ratio of the branching fractions of $D^+ \rightarrow \tau^+\nu_\tau$ and $D^+ \rightarrow \mu^+\nu_\mu$ can be predicted with negligible uncertainty as

$$R_{\tau/\mu} = \frac{\Gamma(D^+ \rightarrow \tau^+\nu_\tau)}{\Gamma(D^+ \rightarrow \mu^+\nu_\mu)} = \frac{M_\tau^2 \left(1 - \frac{M_\tau^2}{M_{D^+}^2}\right)^2}{M_\mu^2 \left(1 - \frac{M_\mu^2}{M_{D^+}^2}\right)^2} = 2.67. \quad (1.2)$$

It is important to note that this expression is independent of G_F , $|V_{cd}|$ and f_{D^+} , while the uncertainties associated with the higher-order corrections and M_{ℓ/D^+} are negligible.

Some new physics models, such as the two-Higgs-doublet model [13, 14], mediated via charged Higgs bosons, or the seesaw mechanism, which involves lepton mixing with Majorana neutrinos [15], may lead to LFU violation. LFU has been comprehensively tested in the B sector by the BaBar, LHCb, and Belle Collaborations [4–9]. However, tests of $\tau\text{-}\mu$ LFU in the charm sector are still limited by the limited knowledge of the $D^+ \rightarrow \tau^+\nu_\tau$ branching fraction. Previously, BESIII reported the most precise measurement of the $D^+ \rightarrow \mu^+\nu_\mu$ branching fraction [10] and the observation of $D^+ \rightarrow \tau^+\nu_\tau$ [11] via $\tau^+ \rightarrow \pi^+\bar{\nu}_\tau$ based on 2.9 fb^{-1} [12] of e^+e^- collision data taken at $\sqrt{s} = 3.773 \text{ GeV}$, resulting in a ratio $R_{\tau/\mu} = 3.21 \pm 0.64 \pm 0.43$. Improved measurements are essential to obtain better knowledge of this ratio and to enable more sensitive LFU tests.

In this paper, we report an improved measurement of $\mathcal{B}(D^+ \rightarrow \tau^+\nu_\tau)$ and $R_{\tau/\mu}$, with an integrated luminosity of 7.9 fb^{-1} data collected at $\sqrt{s} = 3.773 \text{ GeV}$ with the BESIII detector in 2010, 2021 and 2022. The precision is improved by a factor of two compared with the previous BESIII result [11]. Furthermore, based on the measured partial decay width of $D^+ \rightarrow \ell^+\nu_\ell$ ¹, we determine f_{D^+} by taking the $|V_{cd}|$ from the SM global fit [2], and also extract $|V_{cd}|$ taking as input f_{D^+} from lattice quantum chromodynamics (LQCD) calculations [16].

2 BESIII DETECTOR AND MONTE CARLO SIMULATION

The BESIII detector [17] records symmetric e^+e^- collisions provided by the BEPCII storage ring [18] in the center-of-mass energy range from 1.85 to 4.95 GeV, with a peak luminosity of $1.1 \times 10^{33} \text{ cm}^{-2}\text{s}^{-1}$ achieved at $\sqrt{s} = 3.773 \text{ GeV}$. BESIII has collected large data samples in this energy region [19–21]. The cylindrical core of the BESIII detector covers 93% of the full solid angle and consists of a helium-based multilayer drift chamber (MDC), a plastic scintillator time-of-flight system (TOF), and a CsI(Tl) electromagnetic calorimeter (EMC), which are all enclosed in a superconducting solenoidal magnet providing a 1.0 T magnetic field. The solenoid is supported by an octagonal flux-return yoke with resistive

¹The partial decay width is calculated as the measured branching fraction divided by the D^+ lifetime obtained through a global fit [2].

plate counter muon identification modules interleaved with steel. The charged-particle momentum resolution at $1 \text{ GeV}/c$ is 0.5%, and the dE/dx resolution is 6% for electrons from Bhabha scattering. The EMC measures photon energies with a resolution of 2.5% (5%) at 1 GeV in the barrel (end-cap) region. The time resolution in the TOF barrel region is 68 ps, while that in the end-cap region was 110 ps. The end-cap TOF system was upgraded in 2015 using multigap resistive plate chamber technology, providing a time resolution of 60 ps, which benefits 63% of the data used in this analysis [22].

Monte Carlo (MC) simulated data samples produced with a GEANT4-based [23] software package, which includes the geometric description of the BESIII detector and the detector response, are used to determine detection efficiencies and to estimate backgrounds. The simulation models the beam-energy spread and initial-state radiation (ISR) in the e^+e^- annihilations with the generator KKMC [24]. The inclusive MC sample includes the production of $D\bar{D}$ pairs (including quantum coherence for the neutral D channels), the non- $D\bar{D}$ decays of the $\psi(3770)$, the ISR production of the J/ψ and $\psi(3686)$ states, and the continuum processes incorporated in KKMC [24]. All particle decays are modelled with EVTGEN [25] using branching fractions either taken from the Particle Data Group [2], when available, or otherwise estimated with LUNDCHARM [26]. Final-state radiation from charged final-state particles is incorporated using the PHOTOS package [27]. The leptonic decay $D^+ \rightarrow \tau^+\nu_\tau$ is simulated with the SLN model [25].

3 EVENT SELECTION AND DATA ANALYSIS

The analysis uses the double-tag (DT) technique [28]. All the selection criteria follow those adopted in the previous BESIII study [11]. On the single-tag (ST) side, the D^- mesons are reconstructed via the six hadronic decay modes $K^+\pi^-\pi^-$, $K^+\pi^-\pi^-\pi^0$, $K_S^0\pi^-$, $K_S^0\pi^-\pi^0$, and $K_S^0\pi^-\pi^-\pi^+$. On the signal side, the $\tau^+ \rightarrow \pi^+\bar{\nu}_\tau$ process is used to reconstruct $D^+ \rightarrow \tau^+\nu_\tau$ and thereby measure $R_{\tau/\mu}$.

On the ST side, to distinguish the D^- mesons from the combinatorial backgrounds, two variables, the beam-constrained mass $M_{\text{BC}} \equiv \sqrt{E_{\text{beam}}^2 - |\vec{p}_{D^-}|^2}$ and energy difference $\Delta E \equiv E_{D^-} - E_{\text{beam}}$ are defined, where \vec{p}_{D^-} and E_{D^-} are the total reconstructed momentum and energy of the D^- candidate in the e^+e^- center-of-mass frame, and E_{beam} is the calibrated beam energy. For each ST decay mode, if more than one candidate satisfies the above requirements, the one with the smallest value of $|\Delta E|$ is kept for further analyses. The ST yields for data are obtained by a fit to the M_{BC} distributions with MC based signal shapes convolved with double Gaussian functions. The background shape is parametrized by an ARGUS function with free parameters, except for the endpoint, which is fixed at 1.8865 GeV corresponding to E_{beam} . The fits are shown in Fig. 2. The ST efficiencies are determined by analyzing inclusive MC samples. Those candidates with M_{BC} lying within $(1.863, 1.877) \text{ GeV}/c^2$ are retained for the subsequent analysis. The $|\Delta E|$ requirements, ST yields and the ST efficiencies are shown in Table 1.

After the ST event is identified, the remaining tracks which have not been used in the ST-side reconstruction are used to select candidates for the signal process $D^+ \rightarrow \tau^+\nu_\tau, \tau^+ \rightarrow$

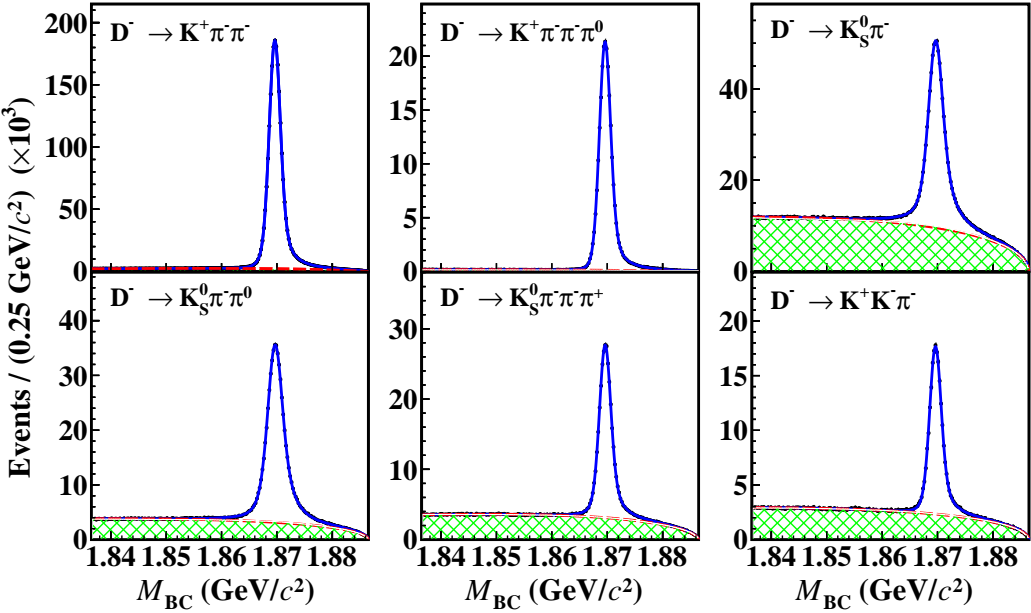


Figure 2. Fits to the M_{BC} distributions of the ST D^- candidates. The dots with error bars are data. The blue solid curves are the fit results. The red dashed curves are the fitted combinatorial backgrounds. The green hatched histograms are background events from the inclusive MC sample.

Table 1. The ΔE requirements, ST yield ($N_{\text{tag}}^{\text{ST}}$) and ST efficiencies ($\epsilon_{\text{tag}}^{\text{ST}}$).

Tag mode	ΔE (MeV)	$N_{\text{tag}}^{\text{ST}}$	$\epsilon_{\text{tag}}^{\text{ST}}(\%)$
$K^+ \pi^- \pi^-$	(-25,24)	2164074 ± 1571	51.17 ± 0.01
$K^+ \pi^- \pi^- \pi^0$	(-57,46)	689042 ± 1172	25.50 ± 0.01
$K_S^0 \pi^-$	(-25,26)	250437 ± 524	50.63 ± 0.02
$K_S^0 \pi^- \pi^0$	(-62,49)	558495 ± 930	26.28 ± 0.01
$K_S^0 \pi^- \pi^- \pi^+$	(-28,27)	300519 ± 669	28.97 ± 0.01
$K^+ K^- \pi^-$	(-24,23)	187379 ± 541	41.06 ± 0.02

$\pi^+ \bar{\nu}_\tau$. Since the neutrinos are not detected, only one charged pion needs to be selected in a candidate event. Hence, we require that there must be only one additional track with opposite charge to the ST side. The selection criteria of the pions are identical to those of the ST side and have to match a shower in the EMC additionally. Since pions and muons are both charged particles with similar masses, the pion selection also accepts muon tracks with comparable efficiency (>90%). However, the deposited energy in the EMC (E_{EMC}) of most muons is less than 300 MeV, which is used to separate muon from pion. To increase the signal significance, we partition the data into a π -like sample with $E_{\text{EMC}} > 300$ MeV and a μ -like sample with $E_{\text{EMC}} \leq 300$ MeV.

Four additional requirements are applied to further suppress background processes. These requirements are set from studies of MC data and the systematic uncertainties are assessed from studies of control samples in the data. (1) Processes with misidentified

electrons backgrounds can contaminate our signal sample, for example the semileptonic decay $D^+ \rightarrow K_L^0 e^+ \nu_e$ when the K_L^0 is missed. The quantity E_{EMC}/p distributes around unity for background processes in this category, where p is the momentum of the track reconstructed in the MDC. Therefore, we require $E_{\text{EMC}}/p < 0.95$ for events in the π -like sample. (2) In order to suppress backgrounds with additional neutral particles, such as $D^+ \rightarrow \eta\pi^+$, we demand $E_{\gamma,\text{max}} < 300$ MeV for both samples, where $E_{\gamma,\text{max}}$ is the maximum energy of all EMC showers not used in the reconstruction of either the ST or DT side. (3) We require $|\cos\theta_{\text{miss}}| < 0.75(0.97)$ for the π -like (μ -like) sample to ensure that the missing track points to the active region of the detector, where $\cos\theta_{\text{miss}}$ is the polar angle of the missing momentum. (4) In order to suppress background from $D^+ \rightarrow K_L^0\pi^+$ decays we impose $\alpha > 45^\circ(25^\circ)$ for the π -like (μ -like) sample, where α is the opening angle between the missing track and the most energetic unassigned shower.

4 DETERMINATION OF THE BRANCHING FRACTION

The quantity missing-mass squared (M_{miss}^2) is defined to provide sensitivity to the missing neutrino:

$$M_{\text{miss}}^2 = (E_{\text{cm}} - E_{D^-} - E_\pi)^2 - (\vec{p}_{\text{cm}} - \vec{p}_{D^-} - \vec{p}_\pi)^2, \quad (4.1)$$

where $E_{\text{cm}}(\vec{p}_{\text{cm}})$ is the center-of-mass energy (momentum), $E_\pi(\vec{p}_\pi)$ is the energy (momentum) of the pion, and $E_{D^-}(\vec{p}_{D^-})$ is the energy (momentum) of the D^- tag. An unbinned simultaneous maximum likelihood fit is performed on the M_{miss}^2 distributions for both the π -like and μ -like samples, shown in Fig. 3, to obtain the yields. The branching fraction of signal process is a common parameter in the fit and is obtained through

$$\mathcal{B}(D^+ \rightarrow \tau^+\nu_\tau) = \frac{N_{\tau\nu}}{\sum_i N_i^{\text{ST}} \epsilon_{i,\tau\nu}^{\text{DT}} / \epsilon_i^{\text{ST}}}, \quad (4.2)$$

where $N_{\tau\nu}$ is the DT yields for all tag modes, $\epsilon_{i,\tau\nu}^{\text{DT}}$ is the signal selection efficiencies without $B(\tau^+ \rightarrow \pi^+\bar{\nu}_\tau)$ shown in Table 2, N_i^{ST} and ϵ_i^{ST} are the numbers of the ST events and ST efficiencies for the ST mode i . In extracting the DT yields for each tag mode the $D^+ \rightarrow \tau^+\nu_\tau$ ($\tau^+ \rightarrow \pi^+\bar{\nu}_\tau$) signal shape is taken from the MC sample. The peaking-background shapes of $D^+ \rightarrow \pi^0\pi^+$ and $D^+ \rightarrow K_L^0\pi^+$ are extracted from data-based control samples. All the other shapes are determined using inclusive MC simulation and constructed using kernel estimation PDF [29] in RooFit [30]. Additionally, the yields of the signal process $D^+ \rightarrow \tau^+\nu_\tau$ ($\tau^+ \rightarrow \pi^+\bar{\nu}_\tau$) and the significant peaking background $D^+ \rightarrow K_L^0\pi^+$ are floated in the fit. The other smaller peaking backgrounds, $D^+ \rightarrow \pi^0\pi^+$, $D^+ \rightarrow \eta\pi^+$, and $D^+ \rightarrow K_S^0\pi^+$ are fixed based on their known branching fractions quoted from the PDG [2] and $D^+ \rightarrow \mu^+\nu_\mu$ quoted from BESIII measurement [10]. The efficiencies obtained by the MC samples. The normalization of the remaining relatively smooth backgrounds is floated, but the relative ratio between π -like and μ -like samples is constrained, based on study of the inclusive MC sample. The $D^+ \rightarrow K_S^0\pi^+$ control sample is used to estimate the difference of data and MC to correct the ratio.

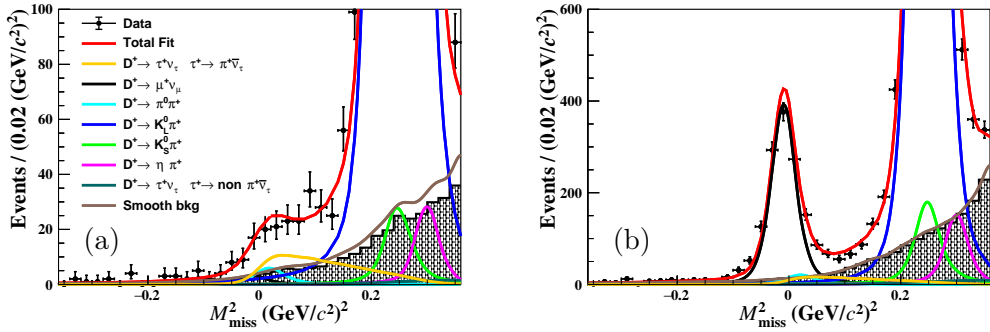


Figure 3. Fits to the distributions of M_{miss}^2 for π -like (a) and μ -like (b) cases. All of the rest of the colored lines correspond to fits to background components.

Table 2. The signal efficiencies ($\epsilon_{\pi(\mu)} = \epsilon_{\pi(\mu)}^{\text{DT}}/\epsilon_{\text{tag}}^{\text{ST}}$) for the $\pi(\mu)$ -like selection. The branching fractions of the sub-particle ($\tau^+ \rightarrow \pi^+ \nu_\tau$) decays are not included. The uncertainties are statistical only.

Tag mode	ϵ_π (%)	ϵ_μ (%)
$D^- \rightarrow K^+ \pi^- \pi^-$	39.54 ± 0.23	25.00 ± 0.19
$D^- \rightarrow K_S^0 \pi^-$	40.48 ± 0.24	25.60 ± 0.19
$D^- \rightarrow K^+ \pi^- \pi^- \pi^0$	38.94 ± 0.33	25.45 ± 0.25
$D^- \rightarrow K_S^0 \pi^- \pi^0$	40.19 ± 0.32	25.07 ± 0.26
$D^- \rightarrow K_S^0 \pi^- \pi^- \pi^+$	37.52 ± 0.31	24.19 ± 0.25
$D^- \rightarrow K^+ K^- \pi^-$	37.74 ± 0.26	23.14 ± 0.20

The signal yield is 283 ± 32 with a statistical significance of 6.5σ . The branching fraction of $D^+ \rightarrow \tau^+ \nu_\tau$ is determined to be $\mathcal{B}(D^+ \rightarrow \tau^+ \nu_\tau) = (9.9 \pm 1.1) \times 10^{-4}$, where the uncertainty is statistical only. As a cross check, we repeat the fit with the yields of $D^+ \rightarrow \mu^+ \nu_\mu$ floated, and obtain $\mathcal{B}(D^+ \rightarrow \tau^+ \nu_\tau) = (1.01 \pm 0.13) \times 10^{-3}$ and $\mathcal{B}(D^+ \rightarrow \mu^+ \nu_\mu) = (3.89 \pm 0.12) \times 10^{-4}$. The latter is consistent with the PDG value of $(3.74 \pm 0.17) \times 10^{-4}$ [2].

5 SYSTEMATIC UNCERTAINTIES

Benefiting from the DT technique, we assume that all systematic uncertainties due to the reconstruction of particles on the ST side largely cancel. The systematic uncertainties are dominated by the selection criteria on the DT side, the simultaneous fit, and the knowledge of $\mathcal{B}(D^+ \rightarrow \mu^+ \nu_\mu)$. These are summarized in Table 3.

The systematic uncertainties associated with the E_{EMC} , E_{EMC}/p and $E_{\gamma, \text{max}}$ requirements are studied using a $D^+ \rightarrow K_S^0 \pi^+$ control sample. Those associated with the $|\cos \theta_{\text{miss}}|$ and missing cone α requirements are estimated by a control sample of $D^0 \rightarrow K^- e^+ \nu_e$ decays. The difference in efficiency of each requirement between data and MC simulation is assigned to be the corresponding systematic uncertainty. To assess the uncertainty associated with the simultaneous fit, we change the MC components for example exclude the non- $D\bar{D}$ process to estimate the effect on the smooth background shapes. We also vary

Table 3. Systematic uncertainties for the branching fraction measurement.

Source	Sys. Uncertainty(%)
E_{EMC} requirement	1.1
Smooth background shape	1.8
π^+ tracking	1.0
π^+ PID	1.0
N_{ST}	0.1
Requirement on E_{EMC}/p	1.1
Requirement on $E_{\gamma,\text{max}}$	1.2
Requirements on $ \cos \theta_{\text{miss}} $ and α	2.9
Tag bias	0.1
Normalizations of small peaking BKG	1.5
Relative size ratio of smooth BKG	1.5
Signal shape of $D^+ \rightarrow \tau^+ \nu_\tau$	0.5
$\mathcal{B}(D^+ \rightarrow \mu^+ \nu_\mu)$	2.1
$\mathcal{B}(\tau^+ \rightarrow \pi^+ \bar{\nu}_\tau)$	0.5
Total	5.2

the E_{EMC} requirement by ± 50 MeV to account for the difference in resolution between data and MC. We vary the normalizations of the small peaking backgrounds $D^+ \rightarrow K_S^0 \pi^+$, $D^+ \rightarrow \pi^0 \pi^+$ and $D^+ \rightarrow \eta \pi^+$ by $\pm 1\sigma$ of their known branching fraction. The ratio of the smooth background contribution between π -like and μ -like samples in the M_{miss}^2 fit has been corrected by $D^+ \rightarrow K_S^0 \pi^+$ control sample and the error is assumed as the systematic uncertainty. We vary the fixed branching fraction of $\mathcal{B}(D^+ \rightarrow \mu^+ \nu_\mu)$ [10] by $\pm 1\sigma$ to estimate the corresponding systematic uncertainty.

6 SUMMARY

Based on e^+e^- collision data corresponding to an integrated luminosity of 7.9 fb^{-1} collected with the BESIII detector at $\sqrt{s} = 3.773 \text{ GeV}$, we measure $\mathcal{B}(D^+ \rightarrow \tau^+ \nu_\tau) = (9.9 \pm 1.1_{\text{stat}} \pm 0.5_{\text{syst}}) \times 10^{-4}$, while fixing $\mathcal{B}(D^+ \rightarrow \mu^+ \nu_\mu) = (3.981 \pm 0.079_{\text{stat}} \pm 0.040_{\text{syst}}) \times 10^{-4}$ [10]. This result is consistent with the previous BESIII measurement of $(1.20 \pm 0.24_{\text{stat}} \pm 0.12_{\text{syst}}) \times 10^{-3}$ [11] and is twice as precise. The ratio $R_{\tau/\mu}$ is determined to be 2.49 ± 0.31 , which is consistent with the SM prediction of 2.67 within one standard deviation.

Table 4. External input parameters with uncertainties.

Parameter	Value
m_μ	$0.10566(24) \text{ GeV}$
m_τ	$1.77686(12) \text{ GeV}$
M_{D^+}	$1.86966(5) \text{ GeV}$
G_F	$1.1663787(6) \times 10^{-5} \text{ GeV}^{-2}$
τ_{D^+}	$1.033(5) \text{ ps}$

Combing the measured branching fraction with the world average value of G_F , m_ℓ , M_{D^+} and the D^+ lifetime (τ_{D^+}) shown in Table 4, we obtain $f_{D^+}|V_{cd}| = (45.9 \pm 2.5_{\text{stat}} \pm 1.2_{\text{syst}} \pm 0.1_{\text{input}})$ MeV. Here the third uncertainty arises from the knowledge of τ_{D^+} (0.2%). Taking the CKM matrix element $|V_{cd}| = 0.22486 \pm 0.00067$ from the global SM fit [2] we obtain $f_{D^+} = (204 \pm 11_{\text{stat}} \pm 5_{\text{syst}} \pm 1_{\text{input}})$ MeV, which is in agreement with the value of $f_{D^+} = (212.1 \pm 0.7)$ MeV from recent LQCD calculations [16]. Alternatively, taking the LQCD value of the decay constant as input, we obtain $|V_{cd}| = (0.216 \pm 0.012_{\text{stat}} \pm 0.006_{\text{syst}} \pm 0.001_{\text{input}})$, which is in agreement with the value from the global SM fit.

Acknowledgement

The BESIII Collaboration thanks the staff of BEPCII and the IHEP computing center for their strong support. This work is supported in part by National Key R&D Program of China under Contracts Nos. 2023YFA1606000, 2020YFA0406400, 2020YFA0406300; National Natural Science Foundation of China (NSFC) under Contracts Nos. 11635010, 11735014, 11935015, 11935016, 11935018, 12025502, 12035009, 12035013, 12061131003, 12192260, 12192261, 12192262, 12192263, 12192264, 12192265, 12221005, 12225509, 12235017, 12361141819, 12305105; the Chinese Academy of Sciences (CAS) Large-Scale Scientific Facility Program; the CAS Center for Excellence in Particle Physics (CCEPP); Joint Large-Scale Scientific Facility Funds of the NSFC and CAS under Contract No. U2032104, U1832207; The Excellent Youth Foundation of Henan Scientific Committee under Contract No. 242300421044; Natural Science Foundation of Shandong Province under Grants No. ZR2023QA119; 100 Talents Program of CAS; The Institute of Nuclear and Particle Physics (INPAC) and Shanghai Key Laboratory for Particle Physics and Cosmology; German Research Foundation DFG under Contracts Nos. FOR5327, GRK 2149; Istituto Nazionale di Fisica Nucleare, Italy; Knut and Alice Wallenberg Foundation under Contracts Nos. 2021.0174, 2021.0299; Ministry of Development of Turkey under Contract No. DPT2006K-120470; National Research Foundation of Korea under Contract No. NRF-2022R1A2C1092335; National Science and Technology fund of Mongolia; National Science Research and Innovation Fund (NSRF) via the Program Management Unit for Human Resources & Institutional Development, Research and Innovation of Thailand under Contracts Nos. B16F640076, B50G670107; Polish National Science Centre under Contract No. 2019/35/O/ST2/02907; Swedish Research Council under Contract No. 2019.04595; The Swedish Foundation for International Cooperation in Research and Higher Education under Contract No. CH2018-7756; U. S. Department of Energy under Contract No. DE-FG02-05ER41374.

References

- [1] B. C. Ke, J. Koponen, H. B. Li and Y. Zheng, [Ann. Rev. Nucl. Part. Sci. **73**, 285-314 \(2023\)](#).
- [2] R. L. Workman *et al.* (Particle Data Group), [Prog. Theor. Exp. Phys. **2022**, 083C01 \(2022\)](#).
- [3] D. Silverman and H. Yao, [Phys. Rev. D **38**, 214 \(1988\)](#).
- [4] J. P. Lees *et al.* (BaBar Collaboration), [Phys. Rev. Lett. **109**, 101802 \(2012\)](#).

- [5] J. P. Lees *et al.* (BaBar Collaboration), *Phys. Rev. D* **88**, 072012 (2013).
- [6] R. Aaij *et al.* (LHCb Collaboration), *Phys. Rev. Lett.* **115**, 111803 (2015).
- [7] R. Aaij *et al.* (LHCb Collaboration), *Phys. Rev. Lett.* **113**, 151601 (2014).
- [8] S. Wehle *et al.* (Belle Collaboration), *Phys. Rev. Lett.* **118**, 111801 (2017).
- [9] R. Aaij *et al.* (LHCb Collaboration), *Phys. Rev. Lett.* **131**, 111802 (2023).
- [10] M. Ablikim *et al.* (BESIII Collaboration), [arXiv:2410.07626 [hep-ex]].
- [11] M. Ablikim *et al.* (BESIII Collaboration), *Phys. Rev. Lett.* **123**, 211802 (2019).
- [12] M. Ablikim (BESIII Collaboration), *Chin. Phys. C* **37**, 123001 (2013).
- [13] S. Fajfer, I. Nisandzic and U. Rojec, *Phys. Rev. D* **91**, 094009 (2015).
- [14] A. G. Akeroyd and C. H. Chen, *Phys. Rev. D* **75**, 075004 (2007).
- [15] G. C. Branco, R. G. Felipe and F. R. Joaquim, *Rev. Mod. Phys.* **84**, 515-565 (2012).
- [16] Y. Aoki *et al.* (Flavour Lattice Averaging Group (FLAG)), *Eur. Phys. J. C* **82**, 869 (2022).
- [17] M. Ablikim *et al.* (BESIII Collaboration), *Nucl. Instrum. Meth. A* **614**, 345 (2010).
- [18] C. H. Yu *et al.*, Proceedings of IPAC2016, Busan, Korea, 2016,
doi:10.18429/JACoW-IPAC2016-TUYA01.
- [19] M. Ablikim *et al.* (BESIII Collaboration), *Chin. Phys. C* **44**, 040001 (2020).
- [20] J. Lu, Y. Xiao, X. Ji, *Radiat. Detect. Technol. Methods* **4**, 337 (2020).
- [21] J. W. Zhang, L. H. Wu, S. S. Sun *et al.*, *Radiat. Detect. Technol. Methods* **6**, 289 (2022).
- [22] X. Li *et al.*, *Radiat. Detect. Technol. Methods* **1**, 13 (2017); Y. X. Guo *et al.*, *Radiat. Detect. Technol. Methods* **1**, 15 (2017); P. Cao *et al.*, *Nucl. Instrum. Meth. A* **953**, 163053 (2020).
- [23] S. Agostinelli *et al.* (GEANT4 Collaboration), *Nucl. Instrum. Meth. A* **506**, 250 (2003).
- [24] S. Jadach, B. F. L. Ward and Z. Was, *Phys. Rev. D* **63**, 113009 (2001); *Comput. Phys. Commun.* **130**, 260 (2000).
- [25] D. J. Lange, *Nucl. Instrum. Meth. A* **462**, 152 (2001); R. G. Ping, *Chin. Phys. C* **32**, 599 (2008).
- [26] J. C. Chen, G. S. Huang, X. R. Qi, D. H. Zhang and Y. S. Zhu, *Phys. Rev. D* **62**, 034003 (2000); R. L. Yang, R. G. Ping and H. Chen, *Chin. Phys. Lett.* **31**, 061301 (2014).
- [27] E. Barberio, B. van Eijk and Z. Was, *Comput. Phys. Commun.* **66**, 115 (1991).
- [28] R. M. Baltrusaitis *et al.* (MARK III Collaboration), *Phys. Rev. Lett.* **56**, 2140 (1986).
J. Adler *et al.* (MARK III Collaboration), *Phys. Rev. Lett.* **60**, 89 (1988).
- [29] K. S. Cranmer, *Comput. Phys. Commun.* **136**, 198-207 (2001).
- [30] P. Canal, B. Bellenot, O. Couet, G. Ganis, P. Mato, L. Moneta, A. Naumann and D. Piparo, *J. Phys. Conf. Ser.* **664**, 062006 (2015).

M. Ablikim¹, M. N. Achasov^{4,c}, P. Adlarson⁷⁶, O. Afedulidis³, X. C. Ai⁸¹, R. Aliberti³⁵,
 A. Amoroso^{75A,75C}, Y. Bai⁵⁷, O. Bakina³⁶, I. Balossino^{29A}, Y. Ban^{46,h}, H.-R. Bao⁶⁴, V. Batozskaya^{1,44},
 K. Begzsuren³², N. Berger³⁵, M. Berlowski⁴⁴, M. Bertani^{28A}, D. Bettoni^{29A}, F. Bianchi^{75A,75C},
 E. Bianco^{75A,75C}, A. Bortone^{75A,75C}, I. Boyko³⁶, R. A. Briere⁵, A. Brueggemann⁶⁹, H. Cai⁷⁷,
 X. Cai^{1,58}, A. Calcaterra^{28A}, G. F. Cao^{1,64}, N. Cao^{1,64}, S. A. Cetin^{62A}, X. Y. Chai^{46,h},
 J. F. Chang^{1,58}, G. R. Che⁴³, Y. Z. Che^{1,58,64}, G. Chelkov^{36,b}, C. Chen⁴³, C. H. Chen⁹,
 Chao Chen⁵⁵, G. Chen¹, H. S. Chen^{1,64}, H. Y. Chen²⁰, M. L. Chen^{1,58,64}, S. J. Chen⁴²,
 S. L. Chen⁴⁵, S. M. Chen⁶¹, T. Chen^{1,64}, X. R. Chen^{31,64}, X. T. Chen^{1,64}, Y. B. Chen^{1,58},
 Y. Q. Chen³⁴, Z. J. Chen^{25,i}, Z. Y. Chen^{1,64}, S. K. Choi¹⁰, G. Cibinetto^{29A}, F. Cossio^{75C},
 J. J. Cui⁵⁰, H. L. Dai^{1,58}, J. P. Dai⁷⁹, A. Dbeysi¹⁸, R. E. de Boer³, D. Dedovich³⁶,
 C. Q. Deng⁷³, Z. Y. Deng¹, A. Denig³⁵, I. Denysenko³⁶, M. Destefanis^{75A,75C}, F. De Mori^{75A,75C},
 B. Ding^{67,1}, X. X. Ding^{46,h}, Y. Ding⁴⁰, Y. Ding³⁴, J. Dong^{1,58}, L. Y. Dong^{1,64}, M. Y. Dong^{1,58,64},
 X. Dong⁷⁷, M. C. Du¹, S. X. Du⁸¹, Y. Y. Duan⁵⁵, Z. H. Duan⁴², P. Egorov^{36,b}, Y. H. Fan⁴⁵,
 J. Fang^{1,58}, J. Fang⁵⁹, S. S. Fang^{1,64}, W. X. Fang¹, Y. Fang¹, Y. Q. Fang^{1,58}, R. Farinelli^{29A},
 L. Fava^{75B,75C}, F. Feldbauer³, G. Felici^{28A}, C. Q. Feng^{72,58}, J. H. Feng⁵⁹, Y. T. Feng^{72,58},
 M. Fritsch³, C. D. Fu¹, J. L. Fu⁶⁴, Y. W. Fu^{1,64}, H. Gao⁶⁴, X. B. Gao⁴¹, Y. N. Gao^{46,h},
 Yang Gao^{72,58}, S. Garbolino^{75C}, I. Garzia^{29A,29B}, L. Ge⁸¹, P. T. Ge¹⁹, Z. W. Ge⁴², C. Geng⁵⁹,
 E. M. Gersabeck⁶⁸, A. Gilman⁷⁰, K. Goetzen¹³, L. Gong⁴⁰, W. X. Gong^{1,58}, W. Gradl³⁵,
 S. Gramigna^{29A,29B}, M. Greco^{75A,75C}, M. H. Gu^{1,58}, Y. T. Gu¹⁵, C. Y. Guan^{1,64}, A. Q. Guo^{31,64},
 L. B. Guo⁴¹, M. J. Guo⁵⁰, R. P. Guo⁴⁹, Y. P. Guo^{12,g}, A. Guskov^{36,b}, J. Gutierrez²⁷,
 K. L. Han⁶⁴, T. T. Han¹, F. Hanisch³, X. Q. Hao¹⁹, F. A. Harris⁶⁶, K. K. He⁵⁵, K. L. He^{1,64},
 F. H. Heinsius³, C. H. Heinz³⁵, Y. K. Heng^{1,58,64}, C. Herold⁶⁰, T. Holtmann³, P. C. Hong³⁴,
 G. Y. Hou^{1,64}, X. T. Hou^{1,64}, Y. R. Hou⁶⁴, Z. L. Hou¹, B. Y. Hu⁵⁹, H. M. Hu^{1,64}, J. F. Hu^{56,j},
 Q. P. Hu^{72,58}, S. L. Hu^{12,g}, T. Hu^{1,58,64}, Y. Hu¹, G. S. Huang^{72,58}, K. X. Huang⁵⁹, L. Q. Huang^{31,64},
 X. T. Huang⁵⁰, Y. P. Huang¹, Y. S. Huang⁵⁹, T. Hussain⁷⁴, F. Hölzken³, N. Hüskens³⁵,
 N. in der Wiesche⁶⁹, J. Jackson²⁷, S. Janchiv³², J. H. Jeong¹⁰, Q. Ji¹, Q. P. Ji¹⁹, W. Ji^{1,64},
 X. B. Ji^{1,64}, X. L. Ji^{1,58}, Y. Y. Ji⁵⁰, X. Q. Jia⁵⁰, Z. K. Jia^{72,58}, D. Jiang^{1,64}, H. B. Jiang⁷⁷,
 P. C. Jiang^{46,h}, S. S. Jiang³⁹, T. J. Jiang¹⁶, X. S. Jiang^{1,58,64}, Y. Jiang⁶⁴, J. B. Jiao⁵⁰,
 J. K. Jiao³⁴, Z. Jiao²³, S. Jin⁴², Y. Jin⁶⁷, M. Q. Jing^{1,64}, X. M. Jing⁶⁴, T. Johansson⁷⁶,
 S. Kabana³³, N. Kalantar-Nayestanaki⁶⁵, X. L. Kang⁹, X. S. Kang⁴⁰, M. Kavatsyuk⁶⁵,
 B. C. Ke⁸¹, V. Khachatryan²⁷, A. Khoukaz⁶⁹, R. Kiuchi¹, O. B. Kolcu^{62A}, B. Kopf³,
 M. Kuessner³, X. Kui^{1,64}, N. Kumar²⁶, A. Kupsc^{44,76}, W. Kühn³⁷, L. Lavezzi^{75A,75C},
 T. T. Lei^{72,58}, Z. H. Lei^{72,58}, M. Lellmann³⁵, T. Lenz³⁵, C. Li⁴⁷, C. Li⁴³, C. H. Li³⁹,
 Cheng Li^{72,58}, D. M. Li⁸¹, F. Li^{1,58}, G. Li¹, H. B. Li^{1,64}, H. J. Li¹⁹, H. N. Li^{56,j}, Hui Li⁴³,
 J. R. Li⁶¹, J. S. Li⁵⁹, K. Li¹, K. L. Li¹⁹, L. J. Li^{1,64}, L. K. Li¹, Lei Li⁴⁸, M. H. Li⁴³,
 P. R. Li^{38,k,l}, Q. M. Li^{1,64}, Q. X. Li⁵⁰, R. Li^{17,31}, S. X. Li¹², T. Li⁵⁰, W. D. Li^{1,64}, W. G. Li^{1,a},
 X. Li^{1,64}, X. H. Li^{72,58}, X. L. Li⁵⁰, X. Y. Li^{1,8}, X. Z. Li⁵⁹, Y. G. Li^{46,h}, Z. J. Li⁵⁹, Z. Y. Li⁷⁹,
 C. Liang⁴², H. Liang^{1,64}, H. Liang^{72,58}, Y. F. Liang⁵⁴, Y. T. Liang^{31,64}, G. R. Liao¹⁴,
 Y. P. Liao^{1,64}, J. Libby²⁶, A. Limphirat⁶⁰, C. C. Lin⁵⁵, C. X. Lin⁶⁴, D. X. Lin^{31,64},
 T. Lin¹, B. J. Liu¹, B. X. Liu⁷⁷, C. Liu³⁴, C. X. Liu¹, F. Liu¹, F. H. Liu⁵³, Feng Liu⁶,
 G. M. Liu^{56,j}, H. Liu^{38,k,l}, H. B. Liu¹⁵, H. H. Liu¹, H. M. Liu^{1,64}, Huihui Liu²¹, J. B. Liu^{72,58},
 J. Y. Liu^{1,64}, K. Liu^{38,k,l}, K. Y. Liu⁴⁰, Ke Liu²², L. Liu^{72,58}, L. C. Liu⁴³, Lu Liu⁴³,
 M. H. Liu^{12,g}, P. L. Liu¹, Q. Liu⁶⁴, S. B. Liu^{72,58}, T. Liu^{12,g}, W. K. Liu⁴³, W. M. Liu^{72,58},

X. Liu³⁹, X. Liu^{38,k,l}, Y. Liu⁸¹, Y. Liu^{38,k,l}, Y. B. Liu⁴³, Z. A. Liu^{1,58,64}, Z. D. Liu⁹,
 Z. Q. Liu⁵⁰, X. C. Lou^{1,58,64}, F. X. Lu⁵⁹, H. J. Lu²³, J. G. Lu^{1,58}, X. L. Lu¹, Y. Lu⁷,
 Y. P. Lu^{1,58}, Z. H. Lu^{1,64}, C. L. Luo⁴¹, J. R. Luo⁵⁹, M. X. Luo⁸⁰, T. Luo^{12,g}, X. L. Luo^{1,58},
 X. R. Lyu⁶⁴, Y. F. Lyu⁴³, F. C. Ma⁴⁰, H. Ma⁷⁹, H. L. Ma¹, J. L. Ma^{1,64}, L. L. Ma⁵⁰,
 L. R. Ma⁶⁷, M. M. Ma^{1,64}, Q. M. Ma¹, R. Q. Ma^{1,64}, T. Ma^{72,58}, X. T. Ma^{1,64}, X. Y. Ma^{1,58},
 Y. M. Ma³¹, F. E. Maas¹⁸, I. MacKay⁷⁰, M. Maggiora^{75A,75C}, S. Malde⁷⁰, Y. J. Mao^{46,h},
 Z. P. Mao¹, S. Marcello^{75A,75C}, Z. X. Meng⁶⁷, J. G. Messchendorp^{13,65}, G. Mezzadri^{29A},
 H. Miao^{1,64}, T. J. Min⁴², R. E. Mitchell²⁷, X. H. Mo^{1,58,64}, B. Moses²⁷, N. Yu. Muchnoi^{4,c},
 J. Muskalla³⁵, Y. Nefedov³⁶, F. Nerling^{18,e}, L. S. Nie²⁰, I. B. Nikolaev^{4,c}, Z. Ning^{1,58},
 S. Nisar^{11,m}, Q. L. Niu^{38,k,l}, W. D. Niu⁵⁵, Y. Niu⁵⁰, S. L. Olsen⁶⁴, S. L. Olsen^{10,64},
 Q. Ouyang^{1,58,64}, S. Pacetti^{28B,28C}, X. Pan⁵⁵, Y. Pan⁵⁷, A. Pathak³⁴, Y. P. Pei^{72,58},
 M. Pelizaeus³, H. P. Peng^{72,58}, Y. Y. Peng^{38,k,l}, K. Peters^{13,e}, J. L. Ping⁴¹, R. G. Ping^{1,64},
 S. Plura³⁵, V. Prasad³³, F. Z. Qi¹, H. Qi^{72,58}, H. R. Qi⁶¹, M. Qi⁴², T. Y. Qi^{12,g}, S. Qian^{1,58},
 W. B. Qian⁶⁴, C. F. Qiao⁶⁴, X. K. Qiao⁸¹, J. J. Qin⁷³, L. Q. Qin¹⁴, L. Y. Qin^{72,58},
 X. P. Qin^{12,g}, X. S. Qin⁵⁰, Z. H. Qin^{1,58}, J. F. Qiu¹, Z. H. Qu⁷³, C. F. Redmer³⁵, K. J. Ren³⁹,
 A. Rivetti^{75C}, M. Rolo^{75C}, G. Rong^{1,64}, Ch. Rosner¹⁸, M. Q. Ruan^{1,58}, S. N. Ruan⁴³,
 N. Salone⁴⁴, A. Sarantsev^{36,d}, Y. Schelhaas³⁵, K. Schoenning⁷⁶, M. Scodeggio^{29A}, K. Y. Shan^{12,g},
 W. Shan²⁴, X. Y. Shan^{72,58}, Z. J. Shang^{38,k,l}, J. F. Shangguan¹⁶, L. G. Shao^{1,64}, M. Shao^{72,58},
 C. P. Shen^{12,g}, H. F. Shen^{1,8}, W. H. Shen⁶⁴, X. Y. Shen^{1,64}, B. A. Shi⁶⁴, H. Shi^{72,58},
 J. L. Shi^{12,g}, J. Y. Shi¹, Q. Q. Shi⁵⁵, S. Y. Shi⁷³, X. Shi^{1,58}, J. J. Song¹⁹, T. Z. Song⁵⁹,
 W. M. Song^{34,1}, Y. J. Song^{12,g}, Y. X. Song^{46,h,n}, S. Sosio^{75A,75C}, S. Spataro^{75A,75C},
 F. Stieler³⁵, S. S. Su⁴⁰, Y. J. Su⁶⁴, G. B. Sun⁷⁷, G. X. Sun¹, H. Sun⁶⁴, H. K. Sun¹, J. F. Sun¹⁹,
 K. Sun⁶¹, L. Sun⁷⁷, S. S. Sun^{1,64}, T. Sun^{51,f}, W. Y. Sun³⁴, Y. Sun⁹, Y. J. Sun^{72,58},
 Y. Z. Sun¹, Z. Q. Sun^{1,64}, Z. T. Sun⁵⁰, C. J. Tang⁵⁴, G. Y. Tang¹, J. Tang⁵⁹, M. Tang^{72,58},
 Y. A. Tang⁷⁷, L. Y. Tao⁷³, Q. T. Tao^{25,i}, M. Tat⁷⁰, J. X. Teng^{72,58}, V. Thoren⁷⁶, W. H. Tian⁵⁹,
 Y. Tian^{31,64}, Z. F. Tian⁷⁷, I. Uman^{62B}, Y. Wan⁵⁵, S. J. Wang⁵⁰, B. Wang¹, B. L. Wang⁶⁴,
 Bo Wang^{72,58}, D. Y. Wang^{46,h}, F. Wang⁷³, H. J. Wang^{38,k,l}, J. J. Wang⁷⁷, J. P. Wang⁵⁰,
 K. Wang^{1,58}, L. L. Wang¹, M. Wang⁵⁰, N. Y. Wang⁶⁴, S. Wang^{12,g}, S. Wang^{38,k,l}, T.
 Wang^{12,g}, T. J. Wang⁴³, W. Wang⁵⁹, W. Wang⁷³, W. P. Wang^{35,58,72,o}, X. Wang^{46,h},
 X. F. Wang^{38,k,l}, X. J. Wang³⁹, X. L. Wang^{12,g}, X. N. Wang¹, Y. Wang⁶¹, Y. D. Wang⁴⁵,
 Y. F. Wang^{1,58,64}, Y. H. Wang^{38,k,l}, Y. L. Wang¹⁹, Y. N. Wang⁴⁵, Y. Q. Wang¹, Yaqian Wang¹⁷,
 Yi Wang⁶¹, Z. Wang^{1,58}, Z. L. Wang⁷³, Z. Y. Wang^{1,64}, Ziyi Wang⁶⁴, D. H. Wei¹⁴,
 F. Weidner⁶⁹, S. P. Wen¹, Y. R. Wen³⁹, U. Wiedner³, G. Wilkinson⁷⁰, M. Wolke⁷⁶, L. Wollenberg³,
 C. Wu³⁹, J. F. Wu^{1,8}, L. H. Wu¹, L. J. Wu^{1,64}, X. Wu^{12,g}, X. H. Wu³⁴, Y. Wu^{72,58},
 Y. H. Wu⁵⁵, Y. J. Wu³¹, Z. Wu^{1,58}, L. Xia^{72,58}, X. M. Xian³⁹, B. H. Xiang^{1,64}, T. Xiang^{46,h},
 D. Xiao^{38,k,l}, G. Y. Xiao⁴², S. Y. Xiao¹, Y. L. Xiao^{12,g}, Z. J. Xiao⁴¹, C. Xie⁴², X. H. Xie^{46,h},
 Y. Xie⁵⁰, Y. G. Xie^{1,58}, Y. H. Xie⁶, Z. P. Xie^{72,58}, T. Y. Xing^{1,64}, C. F. Xu^{1,64}, C. J. Xu⁵⁹,
 G. F. Xu¹, H. Y. Xu^{67,2}, M. Xu^{72,58}, Q. J. Xu¹⁶, Q. N. Xu³⁰, W. Xu¹, W. L. Xu⁶⁷,
 X. P. Xu⁵⁵, Y. Xu⁴⁰, Y. C. Xu⁷⁸, Z. S. Xu⁶⁴, F. Yan^{12,g}, L. Yan^{12,g}, W. B. Yan^{72,58},
 W. C. Yan⁸¹, X. Q. Yan^{1,64}, H. J. Yang^{51,f}, H. L. Yang³⁴, H. X. Yang¹, J. H. Yang⁴²,
 T. Yang¹, Y. Yang^{12,g}, Y. F. Yang^{1,64}, Y. F. Yang⁴³, Y. X. Yang^{1,64}, Z. W. Yang^{38,k,l},
 Z. P. Yao⁵⁰, M. Ye^{1,58}, M. H. Ye⁸, J. H. Yin¹, Junhao Yin⁴³, Z. Y. You⁵⁹, B. X. Yu^{1,58,64},
 C. X. Yu⁴³, G. Yu^{1,64}, J. S. Yu^{25,i}, M. C. Yu⁴⁰, T. Yu⁷³, X. D. Yu^{46,h}, Y. C. Yu⁸¹,

C. Z. Yuan^{1,64}, J. Yuan³⁴, J. Yuan⁴⁵, L. Yuan², S. C. Yuan^{1,64}, Y. Yuan^{1,64}, Z. Y. Yuan⁵⁹, C. X. Yue³⁹, A. A. Zafar⁷⁴, F. R. Zeng⁵⁰, S. H. Zeng^{63A,63B,63C,63D}, X. Zeng^{12,g}, Y. Zeng^{25,i}, Y. J. Zeng^{1,64}, Y. J. Zeng⁵⁹, X. Y. Zhai³⁴, Y. C. Zhai⁵⁰, Y. H. Zhan⁵⁹, A. Q. Zhang^{1,64}, B. L. Zhang^{1,64}, B. X. Zhang¹, D. H. Zhang⁴³, G. Y. Zhang¹⁹, H. Zhang⁸¹, H. Zhang^{72,58}, H. C. Zhang^{1,58,64}, H. H. Zhang⁵⁹, H. H. Zhang³⁴, H. Q. Zhang^{1,58,64}, H. R. Zhang^{72,58}, H. Y. Zhang^{1,58}, J. Zhang⁸¹, J. Zhang⁵⁹, J. J. Zhang⁵², J. L. Zhang²⁰, J. Q. Zhang⁴¹, J. S. Zhang^{12,g}, J. W. Zhang^{1,58,64}, J. X. Zhang^{38,k,l}, J. Y. Zhang¹, J. Z. Zhang^{1,64}, Jianyu Zhang⁶⁴, L. M. Zhang⁶¹, Lei Zhang⁴², P. Zhang^{1,64}, Q. Y. Zhang³⁴, R. Y. Zhang^{38,k,l}, S. H. Zhang^{1,64}, Shulei Zhang^{25,i}, X. M. Zhang¹, X. Y. Zhang⁴⁰, X. Y. Zhang⁵⁰, Y. Zhang¹, Y. Zhang⁷³, Y. T. Zhang⁸¹, Y. H. Zhang^{1,58}, Y. M. Zhang³⁹, Yan Zhang^{72,58}, Z. D. Zhang¹, Z. H. Zhang¹, Z. L. Zhang³⁴, Z. Y. Zhang⁷⁷, Z. Y. Zhang⁴³, Z. Z. Zhang⁴⁵, G. Zhao¹, J. Y. Zhao^{1,64}, J. Z. Zhao^{1,58}, L. Zhao¹, Lei Zhao^{72,58}, M. G. Zhao⁴³, N. Zhao⁷⁹, R. P. Zhao⁶⁴, S. J. Zhao⁸¹, Y. B. Zhao^{1,58}, Y. X. Zhao^{31,64}, Z. G. Zhao^{72,58}, A. Zhemchugov^{36,b}, B. Zheng⁷³, B. M. Zheng³⁴, J. P. Zheng^{1,58}, W. J. Zheng^{1,64}, Y. H. Zheng⁶⁴, B. Zhong⁴¹, X. Zhong⁵⁹, H. Zhou⁵⁰, J. Y. Zhou³⁴, L. P. Zhou^{1,64}, S. Zhou⁶, X. Zhou⁷⁷, X. K. Zhou⁶, X. R. Zhou^{72,58}, X. Y. Zhou³⁹, Y. Z. Zhou^{12,g}, Z. C. Zhou²⁰, A. N. Zhu⁶⁴, J. Zhu⁴³, K. Zhu¹, K. J. Zhu^{1,58,64}, K. S. Zhu^{12,g}, L. Zhu³⁴, L. X. Zhu⁶⁴, S. H. Zhu⁷¹, T. J. Zhu^{12,g}, W. D. Zhu⁴¹, Y. C. Zhu^{72,58}, Z. A. Zhu^{1,64}, J. H. Zou¹, J. Zu^{72,58}

(BESIII Collaboration)

¹ *Institute of High Energy Physics, Beijing 100049, People's Republic of China*

² *Beihang University, Beijing 100191, People's Republic of China*

³ *Bochum Ruhr-University, D-44780 Bochum, Germany*

⁴ *Budker Institute of Nuclear Physics SB RAS (BINP), Novosibirsk 630090, Russia*

⁵ *Carnegie Mellon University, Pittsburgh, Pennsylvania 15213, USA*

⁶ *Central China Normal University, Wuhan 430079, People's Republic of China*

⁷ *Central South University, Changsha 410083, People's Republic of China*

⁸ *China Center of Advanced Science and Technology, Beijing 100190, People's Republic of China*

⁹ *China University of Geosciences, Wuhan 430074, People's Republic of China*

¹⁰ *Chung-Ang University, Seoul, 06974, Republic of Korea*

¹¹ *COMSATS University Islamabad, Lahore Campus, Defence Road, Off Raiwind Road, 54000 Lahore, Pakistan*

¹² *Fudan University, Shanghai 200433, People's Republic of China*

¹³ *GSI Helmholtzcentre for Heavy Ion Research GmbH, D-64291 Darmstadt, Germany*

¹⁴ *Guangxi Normal University, Guilin 541004, People's Republic of China*

¹⁵ *Guangxi University, Nanning 530004, People's Republic of China*

¹⁶ *Hangzhou Normal University, Hangzhou 310036, People's Republic of China*

¹⁷ *Hebei University, Baoding 071002, People's Republic of China*

¹⁸ *Helmholtz Institute Mainz, Staudinger Weg 18, D-55099 Mainz, Germany*

¹⁹ *Henan Normal University, Xinxiang 453007, People's Republic of China*

²⁰ *Henan University, Kaifeng 475004, People's Republic of China*

²¹ *Henan University of Science and Technology, Luoyang 471003, People's Republic of China*

China

- ²² Henan University of Technology, Zhengzhou 450001, People's Republic of China
²³ Huangshan College, Huangshan 245000, People's Republic of China
²⁴ Hunan Normal University, Changsha 410081, People's Republic of China
²⁵ Hunan University, Changsha 410082, People's Republic of China
²⁶ Indian Institute of Technology Madras, Chennai 600036, India
²⁷ Indiana University, Bloomington, Indiana 47405, USA
²⁸ INFN Laboratori Nazionali di Frascati , (A)INFN Laboratori Nazionali di Frascati, I-00044, Frascati, Italy; (B)INFN Sezione di Perugia, I-06100, Perugia, Italy; (C)University of Perugia, I-06100, Perugia, Italy
²⁹ INFN Sezione di Ferrara, (A)INFN Sezione di Ferrara, I-44122, Ferrara, Italy; (B)University of Ferrara, I-44122, Ferrara, Italy
³⁰ Inner Mongolia University, Hohhot 010021, People's Republic of China
³¹ Institute of Modern Physics, Lanzhou 730000, People's Republic of China
³² Institute of Physics and Technology, Peace Avenue 54B, Ulaanbaatar 13330, Mongolia
³³ Instituto de Alta Investigación, Universidad de Tarapacá, Casilla 7D, Arica 1000000, Chile
³⁴ Jilin University, Changchun 130012, People's Republic of China
³⁵ Johannes Gutenberg University of Mainz, Johann-Joachim-Becher-Weg 45, D-55099 Mainz, Germany
³⁶ Joint Institute for Nuclear Research, 141980 Dubna, Moscow region, Russia
³⁷ Justus-Liebig-Universitaet Giessen, II. Physikalisches Institut, Heinrich-Buff-Ring 16, D-35392 Giessen, Germany
³⁸ Lanzhou University, Lanzhou 730000, People's Republic of China
³⁹ Liaoning Normal University, Dalian 116029, People's Republic of China
⁴⁰ Liaoning University, Shenyang 110036, People's Republic of China
⁴¹ Nanjing Normal University, Nanjing 210023, People's Republic of China
⁴² Nanjing University, Nanjing 210093, People's Republic of China
⁴³ Nankai University, Tianjin 300071, People's Republic of China
⁴⁴ National Centre for Nuclear Research, Warsaw 02-093, Poland
⁴⁵ North China Electric Power University, Beijing 102206, People's Republic of China
⁴⁶ Peking University, Beijing 100871, People's Republic of China
⁴⁷ Qufu Normal University, Qufu 273165, People's Republic of China
⁴⁸ Renmin University of China, Beijing 100872, People's Republic of China
⁴⁹ Shandong Normal University, Jinan 250014, People's Republic of China
⁵⁰ Shandong University, Jinan 250100, People's Republic of China
⁵¹ Shanghai Jiao Tong University, Shanghai 200240, People's Republic of China
⁵² Shanxi Normal University, Linfen 041004, People's Republic of China
⁵³ Shanxi University, Taiyuan 030006, People's Republic of China
⁵⁴ Sichuan University, Chengdu 610064, People's Republic of China
⁵⁵ Soochow University, Suzhou 215006, People's Republic of China
⁵⁶ South China Normal University, Guangzhou 510006, People's Republic of China
⁵⁷ Southeast University, Nanjing 211100, People's Republic of China

- ⁵⁸ State Key Laboratory of Particle Detection and Electronics, Beijing 100049, Hefei 230026, People's Republic of China
⁵⁹ Sun Yat-Sen University, Guangzhou 510275, People's Republic of China
⁶⁰ Suranaree University of Technology, University Avenue 111, Nakhon Ratchasima 30000, Thailand
⁶¹ Tsinghua University, Beijing 100084, People's Republic of China
⁶² Turkish Accelerator Center Particle Factory Group, (A)Istinye University, 34010, Istanbul, Turkey; (B)Near East University, Nicosia, North Cyprus, 99138, Mersin 10, Turkey
⁶³ University of Bristol, (A)H H Wills Physics Laboratory; (B)Tyndall Avenue; (C)Bristol; (D)BS8 1TL
⁶⁴ University of Chinese Academy of Sciences, Beijing 100049, People's Republic of China
⁶⁵ University of Groningen, NL-9747 AA Groningen, The Netherlands
⁶⁶ University of Hawaii, Honolulu, Hawaii 96822, USA
⁶⁷ University of Jinan, Jinan 250022, People's Republic of China
⁶⁸ University of Manchester, Oxford Road, Manchester, M13 9PL, United Kingdom
⁶⁹ University of Muenster, Wilhelm-Klemm-Strasse 9, 48149 Muenster, Germany
⁷⁰ University of Oxford, Keble Road, Oxford OX13RH, United Kingdom
⁷¹ University of Science and Technology Liaoning, Anshan 114051, People's Republic of China
⁷² University of Science and Technology of China, Hefei 230026, People's Republic of China
⁷³ University of South China, Hengyang 421001, People's Republic of China
⁷⁴ University of the Punjab, Lahore-54590, Pakistan
⁷⁵ University of Turin and INFN, (A)University of Turin, I-10125, Turin, Italy; (B)University of Eastern Piedmont, I-15121, Alessandria, Italy; (C)INFN, I-10125, Turin, Italy
⁷⁶ Uppsala University, Box 516, SE-75120 Uppsala, Sweden
⁷⁷ Wuhan University, Wuhan 430072, People's Republic of China
⁷⁸ Yantai University, Yantai 264005, People's Republic of China
⁷⁹ Yunnan University, Kunming 650500, People's Republic of China
⁸⁰ Zhejiang University, Hangzhou 310027, People's Republic of China
⁸¹ Zhengzhou University, Zhengzhou 450001, People's Republic of China

^a Deceased

- ^b Also at the Moscow Institute of Physics and Technology, Moscow 141700, Russia
^c Also at the Novosibirsk State University, Novosibirsk, 630090, Russia
^d Also at the NRC "Kurchatov Institute", PNPI, 188300, Gatchina, Russia
^e Also at Goethe University Frankfurt, 60323 Frankfurt am Main, Germany
^f Also at Key Laboratory for Particle Physics, Astrophysics and Cosmology, Ministry of Education; Shanghai Key Laboratory for Particle Physics and Cosmology; Institute of Nuclear and Particle Physics, Shanghai 200240, People's Republic of China
^g Also at Key Laboratory of Nuclear Physics and Ion-beam Application (MOE) and Institute of Modern Physics, Fudan University, Shanghai 200443, People's Republic of China
^h Also at State Key Laboratory of Nuclear Physics and Technology, Peking University, Bei-

jing 100871, People's Republic of China

ⁱ Also at School of Physics and Electronics, Hunan University, Changsha 410082, China

^j Also at Guangdong Provincial Key Laboratory of Nuclear Science, Institute of Quantum Matter, South China Normal University, Guangzhou 510006, China

^k Also at MOE Frontiers Science Center for Rare Isotopes, Lanzhou University, Lanzhou 730000, People's Republic of China

^l Also at Lanzhou Center for Theoretical Physics, Lanzhou University, Lanzhou 730000, People's Republic of China

^m Also at the Department of Mathematical Sciences, IBA, Karachi 75270, Pakistan

ⁿ Also at Ecole Polytechnique Federale de Lausanne (EPFL), CH-1015 Lausanne, Switzerland

^o Also at Helmholtz Institute Mainz, Staudinger Weg 18, D-55099 Mainz, Germany